https://doi.org/10.5194/se-2020-11
Preprint. Discussion started: 19 February 2020


Solid Earth Discussions
Open Access

# The abyssal giant pockmarks of the Black Bahama Escarpment: Relations between structures, fluids and carbonate physiography

Thibault Cavailhes[1], Hervé Gillet[1], Léa Guiastrennec-Faugas[1], Thierry Mulder[1], Vincent Hanquiez[1]

[1] Université de Bordeaux (UMR EPOC – OASU CNRS 5805) Allée Geoffroy Saint-Hilaire CS 50023 33615 Pessac, France

*Correspondence to*: Thibault Cavailhes (thibault.cavailhes@u-bordeaux.fr)

**Abstract.**

This study reports the discovery of ~~spectacular~~ abyssal giant pockmarks located at the toe of the Bahamian carbonate platform, along the Black Bahama structurally-controlled Escarpment (BBE) that exhibits up to 4 km of submarine elevation above the San Salvador Abyssal Plain (SSAP). Analysis of seismic reflection and bathymetric data collected during the *CARAMBAR 2 cruise* revealed the presence of 29 pockmarks; their water depths range from - 4584 m to -4967 m whereas their bathymetric depressions are elliptical in shape, range in diameter from 255 m to 1819 m, and in depth from 30 m to 185 m. The pockmarks alignment trends parallel to the BBE as well as the structural lineaments of the area, exclusively between 2200 and 5000 m from its toe, and overlies a buried carbonate bench in which a high-amplitude seismic anomaly has been detected. The pockmark density interestingly increases where the recognized structural lineaments intersect the BBE.

The aforementioned observations suggest an atypical relationship between the spatial occurrence of the abyssal fluid releases, the carbonate platform tectonic structures, the buried carbonate bench that underlies the hemipelagites in the San Salvador abyssal plain and the physiography of the area. Indeed, the ground water entrance during low-level stands, the dissolution of evaporites by meteoric water, the platform-scale thermal convection and the seawater entrance at the platform edge most probably act in concert to favor the circulation of brines and therefore the corrosion within the Bahamian carbonate platform. These mechanisms are particularly efficient along the structural heterogeneities (i.e. faults and fractures) which act as fluid conduits and control the physiography of the area by maintaining the location of the sedimentary pathways. The dense fluids migrate along the faults towards the BBE free edge and are subsequently trapped into the buried carbonate bench that laterally disappears below the low-permeability deep-sea hemipelagics of the SSAP. In consequence, the trapped corrosive fluids dissolve the carbonates preferentially along the tectonic structures such as the Samana Fracture Zone, at the origin of the BBE curvature and triggers collapse-structures in the overlying fine-grained deposits generating giant pockmarks. This structurally-directed process of dissolution is believed to have played a major role in the BBE 5-6 km erosional retreat and also probably explains the occurrence of plunge pools in the area.

https://doi.org/10.5194/se-2020-11
Preprint. Discussion started: 19 February 2020


Solid Earth Discussions
Open Access

## 1. Introduction

Localizing, describing and understanding the zones of the upper crust where the fluids enter, flow, are stored and leak, are critical to discuss and quantify the geo-bio-chemical fluxes between the lithosphere, the hydrosphere and the atmosphere of the Earth (e.g. Dickens, 2003). Since the 1970's, our 4D-conception of the upper crust fluid circulation has been significantly improved by the description and the analysis of submarine fluid-escape features distribution and morphologies (e.g. King and Mac Lean, 1970; Hornbach et al., 2007). Firstly, seafloor seepages have major impacts on seabed stability, implying potential hazards to offshore infrastructures as well as to coastal infrastructures by changing the failure rock mechanics that potentially leads to submarine escarpment destabilization and possibly to tsunamis (e.g. Orange et al., 2002 and herein references). Secondly, their distribution affine our knowledge of the freshwater distribution, storage and flows in coastal and marine systems where the freshwater supply to cities remains problematic (Garven and Freeze, 1984; Post et al., 2013). Thirdly, fluid-escape features distribution has also helped the oil and gas exploration geologists, which have used their presence to detect offshore seepages related to underlying petroleum systems since the 1930's (Abrams and Segall, 2001). Lastly, long-term seeping fluids through the seafloor has been identified as the primary energy for chemosynthetic benthic ecosystems that currently localize a poorly understood submarine high biomass and productivity (Dando et al., 1991; Ondréas et al., 2005).

*Pockmark definition*

King and Mac Lean (1970) first defined the structures discovered off Nova Scotia as follow "*Pockmarks are cone-shaped depressions… possibly formed by ascending gas or subsurface water leakage from underlying … sediments*". These crater-like features commonly occur in fine-grained sediments, have circular to ellipsoidal depression shapes and can reach up to 4000 m in diameter (Cole et al., 2000; Michaud et al. 2005). They have been observed in all ranges of water depth, from shallow-water environments (e.g. ~ -10 m, Backshall et al., 1979) to deep-sea water (~ -3160 m in Marcon et al., 2014) and are considered as giants pockmarks in the case their diameter is greater than 250 m (Foland et al., 2007; Pilcher and Argent, 2007). They have been recognized in different settings such as open oceanic environment (Michaud et al., 2005), lakes (e.g. Chapron et al., 2004), active margins (Salmi et al., 2011), passive margins (Ondréas et al., 2005), along a volcanic ridge (Michaud et al., 2005), in clastic environments (Sultan et al., 2010), in carbonate environments (Backshall et al., 1979; Betzler et al., 2011) and even proposed for explaining some observed Mars surface circular morphologies (Komatsu et al., 2011). Rare fossil palaeo pockmarks have been described in outcrop studies such as the ~~ones~~ from Cantabria in Spain or the southeast basin of France (e.g. Agirrezabala et al., 2013; Gay et al., 2019).

The fluid sources related to pockmarks commonly originate from shallow subsurface sediments (e.g. Baltzer et al. 2017), dewatering and degassing of the gas-charged seafloor (Agirrezabala et al., 2013), buried salt diapirs (e.g. Taylor et al., 2000; Gay et al., 2019), drowned carbonate banks (e.g. Betzler et al., 2011), buried unconformities (e.g. King and MacLean, 1970), buried sedimentary channels (Picher et al., 2007; Gay et al., 2003; Ondreas et al., 2005), buried Mass Transport Deposits (Bayon et al., 2009) and/or underlying petroleum systems (Pilcher and Argent, 2007). The nature of the involved-fluids can be of various origins such as biogenic gas (e.g. Cole et al., 2000; Marcon et al., 2014), thermogenic gas such as hydrates (Pilcher and Argent, 2007), hydrocarbons

https://doi.org/10.5194/se-2020-11
Preprint. Discussion started: 19 February 2020




seeps and/or sand injectites (Cole et al., 2000), fresh water (Chapron et al., 2004) as well as brines and sulfides (Paull and Neumann, 1987).

The fluid ~~ascending movements giving birth to~~ pockmarks can be favored along structural surfaces or rocky basements (Shaw et al., 1997), through fractures in the sediments (e.g. Marcon et al., 2014) and through fault-zones of different scales (e.g. Sultan et al., 2010; Micallef et al., 2011). Fault-strike pockmarks is the relevant terminology for the linear arrangement of pockmarks along the strike of an underlying buried fault (Pilcher and Argent, 2007) whereas fault hanging-wall pockmarks are located above the footwall cut-offs of a fluid-rich unit (Maestro et al., 2002).

Current-day carbonate platforms are commonly subject to dissolution, corrosion, dolomitization and dedolomitization by fresh and saline groundwater in the first kilometers deep (e.g. Sanford and Konikrow, 1989; Hugues et al., 2007; Wierzbicki et al., 2006). The structural heterogeneities are the most efficient fluids entrance, pathway, storage and seepage available spaces in carbonate rocks, allowing both episodic and persistent subsurface fluid-flows through times and overprinting an anisotropy of hydraulic properties in the system, notably the permeability (Sibson, 1996). At the cm-scale, preexisting fractures and faults control the distribution, the orientation and the intensity of the carbonate dissolution by the circulating brines (defect-driven kinetic reactions); the channelized shape of dissolution targets fractures and zones of structural weakness, preferentially along their strikes (Gouze et al., 2003; Garcia-Rios et al., 2015; Privalov et al., 2019). The structurally-controlled dissolution of carbonates, in particular by brines, is poorly understood and remains to be documented at the km-scale.

The Bahama platform ~~offers~~, ~~within a same succession~~ many reservoir rocks with a wide range of porosities (thick shallow water platform limestones and dolomites), organic matter-rich source rocks (restricted marine limestones) as well as the presence of vertical and lateral seals (thick restricted marine anhydrites and restricted marine halites), all needed for petroleum systems (Walles, 1993). In addition, the Black Bahama Escarpment (BBE) offers a 4 km-high submarine topography that increases the vertical interacting section between groundwater and seawater, where the structural lineaments sharply dissect and controls the submarine physiography. This provides an ideal ~~study~~, case to better constrain a structurally-controlled and dissolved carbonate system at the >km-scale. Indeed, evidences such as significant changes in temperature around faults demonstrate the direct and efficient hydrologic relations between surface and great depths (3500 m) into the platform (Walles, 1993). Drilling and core data show that hydrodynamic alteration processes in carbonates near major fault surfaces create buried dissolution conduits (e.g. 8 meters high, $\phi$ = 100%) at a depth of 4000 meters in the Great Bahama Bank (Walles, 1993). Solution collapse brecciation of dolomite sequences, in response to the dissolution of imbedded anhydrites by corrosive fluids along faults, are suspected to cause those surprising reservoir properties within the platform.

In this paper, (i) we address the distribution, the morphometry and the different mechanisms at the origin of the spectacular abyssal giant pockmarks alignment located at the toe of the BBE (Fig. 1). In doing so, we use the bathymetric/seismic data of CARAMBAR 2.0 scientific cruise (December 2016-January 2017) in order to (ii) document and discuss the interactions between the km-scale structural features of the area, the carbonate platform-scale circulation and the current-day physiography. To our knowledge, pockmarks have never been described on modern sea-floor below the Carbonate Compensation Depth (CCD), in abyssal carbonate contexts (>3000 m of water depth), at the toe of a structurally-controlled mega-carbonate escarpment such as the BBE (> 4 km-high).

https://doi.org/10.5194/se-2020-11
Preprint. Discussion started: 19 February 2020




## 2. Geological setting

### 2.1 Tectonic setting and platform establishment

The Bahamas is a post-rift feature mostly made of a stretched pre-Triassic continental crust (Mullins and Lynts, 1977) where a large carbonate platform developed in the Late Jurassic and Early Cretaceous in response to high carbonate production rates (Freeman-Lynde et al., 1981; Carlo, 1996). The clockwise rotation of the North American continental structural block caused a complex transtensional ocean-continent transition where N-S striking normal basement faults (e.g. Black Plateau) have coexisted with E-W striking pre-Jurassic basement Atlantic Ocean fracture zones (e.g. Blake Spur FZ, Great Abaco FZ; Sheridan, 1974). Since the early Cenozoic, active faulting occurred in response to the tectonic interactions between the southern Cuban orogeny and the Mesozoic-aged tectonic structures (Masaferro et al., 2002; Kindler et al., 2011). Post-Oligocene reactivation of vertical basement faults have been reported by Mullins and Van Buren (1981) in Walker's Cay (northern Bahamas) as well as a Neogene to present-day folding in Santaren anticline (Masaferro et al., 2002) and during the Quaternary~~-aged~~ tectonic tilting ~~using~~ the Sunniland Fracture Zone along the Bahama escarpment (Kindler et al., 2011; Fig. 1a).

### 2.2 Current-day physiography and fluid escape features

The present-day morphology of the Blake Bahama Escarpment (BBE) has an erosional origin (~5-6 km of retreat, up to 4.2 km high), essentially developed during the Cretaceous (Freeman-Lynde and Ryan, 1985) and Tertiary times (Schlager et al., 1984), nevertheless the erosion is probably still active. This erosional retreat overprinted a buried "bench-shaped" morphology exhibiting a relict ~5-6 km-wide flat carbonate surface currently buried by Miocene to Quaternary sediments lying in the San Salvador Abyssal plain (Schlager et al., 1984). Consistently to the Blake Escarpment (10-15 km of retreat), an Oligocene unconformity ($A^u$) is present at the top of the Cretaceous carbonates of the buried-bench and predates the Miocene massive sequences of turbidites and the Quaternary hemipelagites (Paull and Dillon, 1980). Contouritic deposits are present at the toe of the BBE at least since the Oligocene in response to abyssal currents activity Bliefnick et al., 1983; Mulder et al., 2019). The aforementioned erosion at the origin of the BBE would be mainly due to the following mechanisms acting in concert in non-quantified proportion at different times: (i) the circulating saline waters and brines that seep from the base of the escarpment dissolve the carbonates and therefore destabilize the slopes (Walles, 1993; Henderson et al., 1999; Paull and Neumann, 1987), such as described along at least 10% of the Florida carbonate Escarpment base (Paull et al., 1988; Chanton et al., 1991). These are made of 94% of seawater and 6% of dense brines (Chanton et al., 1991) and reach temperatures up to 115°C (Paull and Neumann, 1987). The combination of hydrogen sulfides ($HS^-$) and oxygenated seawater (from the platform slope) favors acids ($H^+$) formation that corrode the toe of the escarpment along open vertical fractures. The slope of the escarpment steepens with depth and inner platform carbonate facies at its base strongly suggest that collapse dismantlement operate~~ in depth~~ in response to brine seeps. (ii) Locally, the tectonic activity related to movements along fracture zones implies rock jointing and slope destabilization (Freeman-Lynde and Ryan, 1985).

https://doi.org/10.5194/se-2020-11
Preprint. Discussion started: 19 February 2020



In contrast, the following mechanisms have been interpreted as non-significant to destabilize the slopes of the BBE: (i) the dissolution by oceanic corrosive water below the CCD (Freeman-Lynde and Ryan, 1985) has been excluded by Peterson, (1966) and Paull and Neumann, (1987). (ii) The removal of sediments at the base of the slope by abyssal currents (Schlager et al., 1984; Freeman-Lynde and Ryan, 1985) has been excluded by Paull and Neumann (1987). Indeed, the authors clearly show evidences for ~~such~~ similar erosional structures along the Florida escarpment where the abyssal currents are clearly absent. In addition, (iii) the bioerosion has probably a very limited impact as argued in Freeman-Lynde and Ryan (1985).

### 2.3 Carbonate platform circulation

Fluid~~s~~ circulation within the Bahamas carbonate platform has operated at different times, involving a wide range of fluid volumes, natures (freshwater, seawater and brines) and mechanisms; this has therefore needed efficient and long-term ~~motors~~ of circulations (Melim and Masaferro, 1997). ~~The~~ fluid~~s~~ circulation in a non-quantified proportion is related to: **(i)** ~~the~~ thermally driven circulation causing density gradients between cold ocean waters and ground~~-~~water~~s~~ of the carbonate platform that are warmed by the geothermal heat flux (Kohout et al., 1977; Whitaker and Smart, 1990). **(ii)** ~~The~~ lateral flow due to an across-the-bank head difference (Whitaker and Smart, 1993; Whitaker et al., 1994) and the reflux of mesosaline brines along the platform (salinity of 38-45 ‰) also cause circulation that have important diagenetic implications such as pervasive secondary dolomitization ~~thanks~~ to the magnesium available in ~~the~~ seawater (Simms, 1984; Whitaker and Smart, 1990). The circulation of saline ground water within carbonate platforms is so called ~~the~~ Kohout convection (Hugues et al., 2007). **(iii)** The topographically-driven meteoric groundwater is probably a key factor efficiently driving fluid-circulation into the carbonate platform, in particular during low level stands (Wilson, 2005). The flooding of the banks at the last-deglaciation also strengthened the thermal convection (Dawans and Sawart, 1988; Whitaker et al., 1994). **(iv)** Jointing eases the dissolution by increasing surface area exposed to corrosive waters (Freeman-Lynde and Ryan, 1985) and most probably enhances the existing circulation by supplying efficient, both structurally porous and permeable km-scale fluid-pathways.

## 3. Methodology and database

New data set was acquired during the Leg 2 of the CARAMBAR 2 cruise from December 2016 to January 2017 onboard the R/V l'Atalante. The survey covered the southern part of Exuma Sound, the Exuma Plateau, the Black Bahama Escarpment (BBE) and the adjacent San Salvador abyssal Plain, including 20.395 km$^2$ of multibeam bathymetry and backscatter and 2149 km of HR seismic profiles. Bathymetry and backscatter data have been obtained using a Konsberg EM122/EM710 multibeam echo sounder, and the high-resolution (HR) multichannel seismic system us~~es~~ a 192 channels steamer and ~~related~~ four 35/35 cu in GI air guns (penetration 1-2.5 s two-way travel time). Pockmarks and structural lineaments have been mapped using their physiographic expressions such as depression, local changes in isobaths trends, as well as their seismic expression where 2D seismic data were available (Fig. 2).

## 4. Results

https://doi.org/10.5194/se-2020-11
Preprint. Discussion started: 19 February 2020




### 4.1 Submarine current-day physiography

The studied area is located on an ocean-continent transition that has been as a transforming ocean-continent passive margin (Mullins et al., 1992; Fig. 1a). The Sunniland Fracture Zone (SFZ) bounding the San Salvador Abyssal Plain (SSAP) is parallel to the oceanic paleotransform faults identified on the sea floor of the North Atlantic Plate (NAP); this major transform tectonic corridor trends perpendicular to the magnetic anomalies of the oceanic crust and sharply controls the Eastern side of the Bahamas submarine physiography (Fig. 1a). Only few morphologies and reliefs of the studied area are simply parallel to the N-S striking tensional basement faults recognized in Sheridan's works (1974) that control the Black Plateau area shape.

Based on the analysis of bathymetric maps, the Drowned Barrier Reef (DBR), the Exuma Canyon (EC), the Samana Reentrant (SR), the Exuma Valley (EV), the Exuma Plateau (EP), the South Exuma Plateau Valley (SEPV), the Crooked Canyon (CC), the BBE, the *plunge pools*, and the contouritic deposits have been named consistently to Mulder et al. (2019) (Fig.1b). The generally N-S trending carbonate BBE can reach up to 4200 m of submarine elevation above the San Salvador Abyssal Plain (SSAP) and exhibits an 18 km long curvature located at ~74°10'W; 23.32'N. The BBE curvature is exactly located ~~at the~~ intersection between the SFZ and the BBE. The SFZ appears to be made of different sets of tectonic features striking N110, N145 and E-W (upper right corner of the figure 1b). The 090E structural lineaments orientation definitely controls the shape of the southern part of the BBE, the northern edge of the Samana Reentrant, the EV and the SEPV. The N110 and N145 trending lineaments (mean ~N130 direction) control the submarine morphologies of the southern edge of the Samana Reentrant (SR), the transition between the EV and the SR, as well as the NW-SE trending BBE curvature (Fig. 1b). Regarding the oceanic crust structure ~~in~~ the SSAP, the lineaments are mostly N160 to N-S oriented and controls the elongation of the distal lows where sediments are preferentially deposited (right part of the Figure 1b). In addition, the N-S basement-inherited BBE trend is very similar to the Crooked Canyon orientation. The contourites are present at the toe of the BBE (e.g. Fig. 2a and 2b) with the exception of the BBE curvature area (Fig. 2c).

Summarizing these observations, the physiographic sketches of figure 1b reveals that ocean-continent transition inherited structural lineaments control the BBE trends and curvatures, the submarine giant canyon orientations (Mulder et al., 2019) as well as the abyssal topographies, clearly expressed by the structurally-controlled isobaths contours. This is consistent with the conceptual view of Sheridan (1974) arguing for the presence of structural blocks individualizing the Atlantic continental margin by N-S tensional faults and major strike-slip features accommodating block rotation.

### 4.2 Pockmark Regional distribution

29 abyssal pockmarks have been mapped at the toe of the BBE, in the western part of the SSAP lying at ~ - 4900 m of depth (Fig.1b and 2); they occupy ~20% of the base of the carbonate escarpment, i.e. a total of 21.5 km / 102 km long (Fig.1b). Pockmarks depths range from - 4584 m to - 4967 m, exclusively underneath the Carbonate Compensation Depth of the area (~ - 4500 m; Heath and Mullins, 1984) (Fig. 2; Table 1). They are spectacularly all located between 2 km and 5 km seaward of the toe of the BBE (isobath - 4000m). The mean pockmark diameters range from 255 m to 1819 m and form depressions ranging from 30 m to 185 m of depth without any clear preferential direction of elongation (refer to the *4.4 section* for details). The pockmarks of this study (29/29) are so called giant pockmarks considering their diameters wider than 250 m, following the

https://doi.org/10.5194/se-2020-11
Preprint. Discussion started: 19 February 2020



classification of Foland et al., (1999). Pockmarks are not randomly distributed in the studied area and show a high concentration nearby the BBE curvature (Fig. 1b and 2c). Pockmarks density increases at the vicinity of the BBE curvature where (i) the structural lineaments of the SFZ intersect the BBE and (ii) where the contouritic deposits are absent. The pockmarks have been classified in two families: the inner pockmarks (n=7; $d_{escarpment}$ = 2 - 3 km) and the outer pockmarks (n=22; $d_{escarpment}$ = 3 - 5 km). In order to facilitate the description of the bathymetric map (Fig.1 and 2), the pockmarks have been numbered from the south to the north (Fig. 2a to 2d); In the case of 14a, 14b, 17a and 17b, each couple of overlapping pockmarks have the same number. . This study therefore distinguishes four areas of interest where a detailed analysis of abyssal pockmarks is proposed (Fig. 2a, b, c and d).

Pockmark 1 is located in contouritic deposits and clearly appears isolated from the other pockmarks (around 7 km southwards the pockmark 2; Fig.2a and 2b). It seems aligned with the E-W trending structural lineament bounding the north of the EC and the southern *plunge pool* recognized in Mulder et al. (2019) (Fig. 1b). This is also, with the pockmarks 23 to 27, one of the pockmarks of the study piercing contouritic deposits.

Pockmarks 2, 4, 6, 7 and to 8 appear to be N-S aligned and located at ~3500 m from the BBE (Fig. 2b). In contrast, the pockmarks 3 and 5 are 1000 m to 2000 m closer to the BBE than 2, 4, 6, and 7. We so call these pockmarks, inner pockmarks (Fig. 2b). The spacing between the pockmarks is comprised between 0 m for the overlapping pockmarks (i.e. #7 and #8) and 1200 m (i.e. #2 and #4).

Pockmarks 9, 10, 11, 12, 13, 14a, 14b, 15, 16, 17a, 17b, 18, 19, 20 and 21 are located within the BBE curvature (~74°10'W; 23.32'N; (Fig. 2c). More than half of the studied pockmarks (15/29) are therefore located in the BBE curvature where structural lineaments cross the BBE. Pockmarks 14a, 14b, 17a and 17b are called inner pockmarks because they are located at 2709 m and 2838 m from the BBE (Table 1). In contrast, the other pockmarks form a chain more distant to the BBE (around 4000 m; Fig. 2c). Contouritic deposits seems to be absent from this area (Fig. 1b). Pockmark density is maximum in this area.

Pockmarks 22, 23, 24, 25, 26 and 27 are located in the northern part of the studied area where a contouritic body has been mapped (Fig. 1b). The pockmarks water depths range from -4710 m to -4812 m whereas the inner pockmark 26 is located at only 2211 m from the BBE, which contrasts with the others located at around 4000 m from the BBE (Fig. 2d).

### 4.3 Vertical architecture and pockmarks

The geological detailed interpretations of seismic profiles in figure 3 are given in figure 4: Both figures have to be read simultaneously. The figure 3a, 3b, 3c, 3d, 3e and 3f respectively correspond to the figure 4a, 4b, 4c, 4d, 4e and 4f. These figures exhibits two BBE-perpendicular-trending seismic lines (Fig.3a, 4a and 3d, 4d) and one single BBE-parallel trending seismic line (Fig. 3b and 4b), which are all localized in Figure 1.

*Sedimentary reflectors* – The offshore seismic reflectors are believed to exhibit respectively from the subsurface to the surface, the top of the oceanic crust (basement), the top Kimmeridgian sedimentary package and the top of the Tithonian sedimentary package, consistently with the work of Schlager et al. (1984) (Fig. 3a and 4a). These interpreted sedimentary packages are westwards dipping and thickening, despite the fact their clear seismic expressions is blurring towards the BBE. The oceanic crust is around 0.3 s TWT deep in the eastern part of the profile whereas it is 1.2 s TWT deep in the western part of the profile. Due to this basement structural dip and the high sedimentary supply nearby the platform, the thickness of the sedimentary package is maximum at the toe of the BBE. The Oligocene unconformity ($A^u$) has also been identified due to its high-amplitude seismic reflections as well as the recognized "downlaps" in the overlying Miocene deep-sea deposits (Fig. 3a and 4a; Paull and Dillon, 1980).

*Buried bench* - A 6 km wide buried carbonate bench exhibiting a typical blind facies is clearly identifiable in figures 3a and 3d and is similar to the one described for the area (Schlager et al., 1984). The top of this structure is located at around 6.5 s TWT and is overlain by contouritic deposits (Fig. 3a, 4a), except in the BBE curvature surrounding where it lies under a few 200 to 300 ms thick toe of slope hemipelagic cover (Fig. 3d, 3f, 4d and 4f). The seismic signal expression of the bench is also similar to the wider one (10-15 km) recognized at the toe of the Black Escarpment (Paull and Dillon, 1980). Subvertical seismic discontinuities within the bench suggest the presence of well-defined linear, antithetic and therefore "brittle-stylized" collapse faults (Fig. 4c) that have interestingly a "softer" shape in the overlying contouritic body, this latter being probably less lithified than the bench carbonates.

*Bright spot* - The BBE - parallel seismic line crosses twice the BBE and exhibits diffusive high amplitude seismic anomalies (bright spot) between 6.4 s and 7.0 s TWT. The depth of this feature is independent of the seafloor water depth or relief, therefore demonstrating that this feature originates from subsurface processes (Fig. 3b, 4b). The perpendicular trending seismic line exhibits a V-Shape structure (cone of deformation) which is located right above the buried carbonate bench and terminates on the flank of the pockmark #1. The V-Shape structure is given by antithetic normal faults with sub seismic offsets that form a network apparently accommodating downwards collapse movement (Fig. 3c; 4c)The base of the V-shaped structure is located within the bench (Fig. 3c, 4c), between 0.6 s and 0.9 s underneath the seafloor depression. This bucket-shaped seismic bright spot shows a significant contrast between high-amplitude layered facies recognized in its upper part, the chaotic facies identified at its base and the low amplitude reflectors in the surrounding sedimentary rocks (Fig. 3c, 4c).

*Contourites* – The fine-grained deep-sea hemipelagics materializes the contouritic body and are crosscut by the pockmark #1 depression (fig. 3c). This depression is bounded by at least four anthithetic curved normal faults and shows a chaotic/disorganized facies in its center. The flanks of the pockmarks, made of at least three packages of contourite deposits, show increasing sedimentary thicknesses at the vicinity of the depression (Fig. 4c). At least the upper package exhibits a hyperbolized seismic facies interpreted as a potential flank destabilization (zoom on fig. 4c).

The 23$^{th}$ of December 2016 (20h13 - 20h23 UT), we recorded with the multibeam echosounder the acoustic response in the water column, in the frame of the Carambar 2 cruise. There was no evidence for acoustic anomalies (fluid plum) in the overlying water columns of the pockmark #1 as well as the 28$^{th}$ of December (15h34 - 15h47 UT), within the water column of the pockmark #15,

**4.4 Quantitative analysis**

Water depths for the studied pockmarks are comprised between -4584 m and -4967 m (Fig. 5a). The deepest pockmarks are located within the BBE curvature where contouritic deposits are absent. The shallowest pockmark is the southern one (1) that is perched on contouritic deposits and isolated (-4584 m). The inner pockmarks at the vicinity of the BBE curvature (i.e. 14a, 14b, 17a, 17b) are clearly shallower than the outer ones

https://doi.org/10.5194/se-2020-11
Preprint. Discussion started: 19 February 2020



(9, 10, 11, 12, 13, 15, 16, 18, 19, 20, and 21). Consistently, the inner pockmark 26 is shallower than the 24, 25 and 27 outer ones.

All the giant pockmarks of this study are located between 2211 m (#26) and 4648 m (#25) away from isobath "- 4000 m" expressing the toe of BBE in this study (Fig. 5b). The 7 inner pockmarks are located between 2211 m (#26) and 2894 m (#3) from the BBE whereas the outer pockmarks are located between 2943 m (#9) and 4648 m (#25). The greatest distances between the BBE and the outer pockmarks are systematically less than the BBE erosional retreat (5-6 km) proposed in Freeman-Lynde and Ryan, (1985) and Schlager et al. (1980). Pockmarks appear to be always located right above the buried carbonate bench.

Pockmark mean diameters and pockmark shortest distances to the BBE appear dependent according to the positive correlation of the figure 5c. Two main trends can be individualized on this graph, both including inner and outer pockmarks. For both relations, closer from the BBE is the pockmark, smaller it is.

Pockmarks elongations have been measured for outer and inner pockmarks (Fig. 5d). Most of the pockmarks are slightly elongated with the exception of the inner pockmark #5, which probably originated from several underlying coalescent pockmarks. The related rose diagram highlights a slight N-S preferential direction of elongation (Fig. 5d). The inner pockmarks seem to be generally smaller than the outer ones.

The pockmark depression depths positively correlate with the pockmark mean diameters (Fig. 5e). The pockmark depression depths seem to be around 1/10 of the pockmark mean diameters. This scaling law is consistent with the results from Pilcher and Argent (2007).

## 5. Interpretations and discussion

The physiographic sketch in figure 1 highlights that structural lineaments have most probably controlled and localized through times persistent and well-defined sedimentary pathways from the platform to the San Salvador abyssal plain such as the Great Abaco Canyon (Mulder et al., 2018; 2019). The studied fluid escape features (pockmarks) occupies 20% of the BBE toe and are preferentially localized at the intersection between the BBE and the inherited structural lineaments of the area (Fig. 1a). These observations demonstrate that structurally-driven fluid circulation along the lineaments and through the carbonate platform has probably played a key role during the erosional process leading to the retreat of the BBE. The deep-sea release of fluids have most likely corroded and destabilized the platform toe which is supported by the direct observations that this type of carbonate escarpments currently exhibits unstable submarine slopes steepening with depth (Paull and Neumann, 1987; Fig. 6). The BBE erosional retreat has therefore preferentially reused the inherited faults initially formed by the existing transforming Continent-Ocean-Transition (COT) to reach its present shape (Fig. 6a).

In this part of the manuscript, we (i) hierarchize the importance of the different controlling parameters explaining the pockmarks locations and we discuss (ii) the fluid origin, (iii) the platform-scale circulation, (iv) the timing for pockmark activity as well as the (v) the probable triggering/enhancing mechanisms for fluid releases. The structural, physical, chemical and time modalities leading to the current-day observed abyssal physiography are also discussed.

### 5.1 Controlling parameters for pockmark regional distribution

https://doi.org/10.5194/se-2020-11
Preprint. Discussion started: 19 February 2020




#### 5.1.1. The distance to the BBE (first-order)

All the discovered pockmarks are located at less than 4.7 km from the toe of the BBE, in this study expressed by the isobath – 4000 m (Fig. 5b). 6 km is the width of the buried carbonate bench described in Schlager et al. (1984) that is consistent with the amount of 5-6 km of erosional retreat proposed in Freeman-Lynde and Ryan (1985). In this study, the 2D – seismic lines analysis corroborated that the aforementioned buried carbonate bench is present all over the area and in particular underneath the studied giant pockmarks (e.g. Fig. 4d). These results highlight the close genetic relationship between (i) the toe of the escarpment, (ii) the pockmarks occurrence and (iii) the presence of carbonate bench. Moreover, an N-S elongated pockmark-underlying-seismic-anomaly (high amplitude) appears to be located into the buried carbonate bench (e.g. Fig. 3b, 4b). Thanks to the high quality of the acquired data, we here propose that the fluids at the origin of the studied abyssal giant pockmarks are currently expressed by the recognized underlying high-amplitude seismic anomalies (Fig. 3c), and originate from the buried carbonate bench.

#### 5.1.2 The regional faults (second-order)

The highest density of pockmarks has been identified where the BBE is structurally controlled by the Sunniland Fracture Zone (SFZ; Kindler et al., 2011), leading to the BBE curvature (23°30’0’’N in figure 1b, pockmarks #9 to #21 in figure 5a). This fact implies a causal connection between pockmarks location and structural lineaments in which the focused fluid migration is much more effective than non-focused flow through matrix porosities of the carbonate sedimentary column (Fig. 1; e.g. Abrams, 1992). The permeability of fracture corridors in carbonates, so called structural porosity, is commonly higher than the matrix permeability (e.g. Rotevatn and Bastesen, 2014); This is coherent with the preferential pathways used by the fluids to pop up of the buried bench (Fig. 6b). Strike-slip faults are more efficient to drain fluids along a vertical direction (Cavailhes et al., 2013) that is consistent with the SFZ inherited architecture which is considered as an inherited strike-slip tectonic structure (transform faults) related to the Atlantic ocean opening. In addition, Privalov et al. (2019) showed that, at the plug scale, dissolution and corrosion in carbonates are both eased and preferentially localized along fractures, along which cavities more easily form and grow. These structural heterogeneities are here expressed at the big scale by the structural lineaments that control the dissolution distribution at the platform scale.

The studied pockmarks show at least three morphometric similarities (i.e. diameter, water depth (- *4485 m; -4058 m)* and presence along a structural lineament) with the *plunge pools* succinctly described in Mulder et al. (2018) (Fig. 1). These latter only differ in terms of (i) location in the geological system i.e., located into the platform incising canyon and (ii) the depression depth (> 300 m). Unfortunately, we did not collect 2D seismic-lines crossing the *plunge pools*. However, a partial explanation for *plunge pools* static emplacement into the canyon (through times) could be the presence of an underlying cavity (doline-like feature) related to an underlying structurally-controlled preferential dissolution/corrosion along a preexisting tectonic structure.

#### 5.1.3 Contourites, oceanic currents and buried sedimentary bodies (third-order)

Pockmarks can be present whether contouritic deposits are present or absent, therefore demonstrating that abyssal contouritic deposits did not inhibit the fluid-escape piercing at the toe of the BBE. In contrast, in the areas where the contouritic deposits are absent (e.g. #9 to #21, Fig. 2c), the pockmarks number is higher than in the areas where the contourites are present (e.g. #1, Fig. 2a). In addition, the figure 4c shows that the pockmark #1 growth and probable related fluid-release both occur during a multi-stages building of contourite bodies. These observations would suggest that the contourites establishment (that is synchronous with the pockmark formation) has an impact on the pockmarks field development in controlling the numbers of pockmarks in a given area. This is consistent with the literature in which contourites are commonly considered as a seal for fluid escape structures (Sun et al., 2010). The studied pockmarks are elliptical in shape (Fig. 4) without any clear relation with the southwards stream bottom direction of the Deep Western Boundary Current (Meinen et al., 2013). This means that based on our data, abyssal currents did not modify the studied pockmarks geometric shapes (Andersen et al., 2008; Michel et al., 2017). Post-pockmark contourites may also hide some underlying buried pockmarks, not identified on neither 2D seismic lines nor on bathymetric map. Based on our 2D seismic analysis, no underlying buried sedimentary channels have been recognized underneath the abyssal mega-pockmarks of this study. This means that there is no additional buried sedimentary body at the origin of the storage and release of fluids with the exception of the carbonate bench.

## 5.2 Fluid origin and platform-scale circulation

### 5.2.1 Relation between the source depth and the pockmark diameter

The inner pockmarks mean diameters are smaller than the outer pockmarks ones (Fig. 5c). This observation suggests a particular geometric relation between the pockmark diameters and their distances to the BBE. Indeed, shallower the underlying source is located (overpressure location), smaller should be the pockmark diameter because the collapse structure is bounded by normal faults (Fig. 6b). In consequence, we propose that the top of the buried bench, trapping the fluids, exhibits its own eastwards dipping slope, probably acquired during the Oligocene erosion phase (Paull and Dillon, 1980). Assuming a similar pockmark collapse faults dips for all cases (either 60°, 70° or 80° in the figure 6d) and using the theorem of Pythagoras, we propose to quantitatively estimate the depth of the overpressure location for the inner pockmarks. The base of the seismic anomaly where the pockmark 1 roots is located at ~0.9 s below the seafloor i.e. 882 m - 1035 m in depth, assuming Vp velocities in the range of 1.96-2.30 km/s (Hollister et al., 1972a; Hollister et al., 1972b). These estimations seem consistent with a depth of ~ 1 km inferred from the 60° dipping normal faults (Anderson, 1951; Fig. 6c) commonly bounding collapsing structures such as sketched in usual pockmark models (Gay et al., 2017).

### 5.2.2 Fluid circulation at the Platform scale

The purpose of this section is to qualitatively describe and synthetize the architecture and the mechanisms of the fluid circulation in the Carbonate Bahama Platform (Fig. 7a). Surface seawater and meteoric waters both enter into faults and fracture corridors of the Bahamas platform hosting carbonates (limestone, dolomite) and evaporites (anhydrites, halites) (Fig. 7d). They form a ~1 km-deep meteoric aquifer in which part of the storage is matrix-located whereas freshwater supplies are most probably structurally guided; indeed, fresh water has been for instance recognized at ~3600 m of depth into the Great Bahama Bank (Walles, 1993; Fig.7a). Anhydrites such as the Cedar Key formation (Chanton et al., 1991) can be located at ~1 km depth into the platform (Hugues et al., 2007) and have a transitory barrier effect on the downwards fluid flow, efficiently compartmentalizing most of the fresh water aquifer circulation into the first kilometer. A fraction of this water dissolves these anhydrites,

https://doi.org/10.5194/se-2020-11
Preprint. Discussion started: 19 February 2020



increasing sulfates content in waters as well as water densities; this consequently enhances the water downwards movement into the Bahamas platform. These brines-rich waters ($SO4^{2-}$) are subsequently heated by thermal flux (e.g. 113°C at 4.6 km of depth; Chanton et al., 1991) generating formation of brines rich in sulfides ($S^{2-}$) and containing thermogenic methane ($CH_4$)(Fig.7b). These fluids migrate horizontally eastwards to the free edge of the Bahamian platform (~10.6 cm $an^{-1}$; Henderson et al.1999), along the relatively high-permeability faults and fractures systems (Fig. 7a; e.g., Sunniland Fracture Zone). In the BBE mixed water zone, the cold and oxygenated seawater microbially reduces sulfates ($SO_4^{2-}$) to sulfides ($S^{2-}$). Seawater and brines both keep on flowing through the structural heterogeneities, towards the bench, due their abnormal high density. They are subsequently "trapped" into the bench where the host-rock platform carbonates facies laterally and vertically changes to low-permeability hemipelagic deposits. This phenomenon results in an identified area of mixed chemistry (Fig. 7b) and relative fluid overpressure where the dissolution is probably over-developed (Corbella et al., 2004). The fluids are probably episodically expelled through the top of the bench - which is pre-fractured by the structural lineaments whereas its pressure occasionally exceeds the pressure of the overlying hemipelagics top-seal capillarity. A "doline-like-feature" takes place at the top of the carbonate bench (Oligocene $A^u$-unconformity), implying an overlying pockmark as a surface expression of fluid-escapes in fine-grained sediments (Fig. 7a). These energy-rich fluids may fuel chemosynthetic food chains such as shown in Chanton et al. (1991); however, we do not have any data for discussing such food chains in the study area. Fluid-escape features that have been recognized by Paull and Neumann (1987) are decametric in scale whereas the mega-pockmarks of this study are 10 to 100 times larger. This is consistent with the model of Gay et al. (2019) showing sporadic decametric seeps within a giant pockmark depression that act at different times as a function of available pathways in the sedimentary column and imply fluids lateral migration.

### 5.3 Timing of activity, triggering and enhancing mechanisms

During the CARAMBAR 2 survey, there was no evidence for acoustic anomalies in the overlying-pockmark water columns (#1 and #15). This suggests that no fluid was presently leaking from the pockmarks #1 and #15. However, the seismic anomaly recognized into the buried carbonate bench suggests that the fluids were present, at a non-evaluated pressure (Fig. 3c; 4c). As stated in the introduction, the following mechanisms probably play a role in a non-quantified proportion, at different times-scales enumerated as follows:

(i) At the geologic time-scale, Kohout convection drives the platform fluid circulation (Morrow, 1998). Modelling suggests that the inflow of seawater within carbonate platforms would be similar without the heat flux; however, this latter tends to reduce the asymmetry of circulation (Hughes et al., 2007).

(ii) At the Milankovich timescales, topography-driven flow can also enhance the platform circulation (Garven, 1995; Swennen et al., 2013) by the input of additional fresh water into the platform during the low-level stands (Hughes et al., 2007). Indeed, the large emerged Bahamas Platform (until/to -6000 years, Fauquembergue et al., 2018) probably supplied more fresh water in the underlying system than during the high sea level periods. This enhances the underlying dissolution by increasing chemical disequilibrium into the platform, implying significant source ratio changes in the underlying aquifer between brines, fresh water and meteoric waters. In

https://doi.org/10.5194/se-2020-11
Preprint. Discussion started: 19 February 2020



addition, episodic fluid releases can also be directly related to the decrease of the overlying water column height above the pockmark during low level stands (Riboulot et al., 2014).

(iii) The erosion of the overlying contouritic body by an abyssal current, such as the WBUC (Meinen et al., 2013), can facilitate pockmark formation or activity. Indeed, the removal of this overlying material would change the pressure state of the underlying system (depressurization), therefore triggering a fluid release.

(iv) Earthquakes and volcanic eruptions occurrences have been correlated to tides (Kasahara, 2002) whereas their highest severity occurs when the tidal forces are the strongest (Glaser, 2004). Submarine earthquakes occurrence along deep mid-oceanic ridges (> - 2000 m) has been related to low tides when ocean loading is at a minimum (Tolstoy et al., 2002). The logic would be that fluids escaping from a pockmark-underlying chamber mechanically respond in the same way during low tides and associated depressurization. This has been corroborated for shallow water pockmarks affecting bioclastic carbonates where a relationship between seeps, tidal cycles and possibly atmospheric cyclonic lows is proposed (Rollet et al., 2006). The total water pressure generates a difference in interstitial pore pressure, which allows the expulsion of gas. However, for abyssal pockmarks, this pressure change could be negligible comparing to a pressure of 4500 m – high water column.

(v) Earthquake-induced circulation such as seismic pumping may have played a role in the system (Sibson, 1996). Earthquakes could also destabilize the hemipelagics top sealing properties by slope failures and submarine landslides (Masafero et al., 2011).

(vi) Quaternary tectonic tilting using the Sunniland Fracture Zone along the Bahama Escarpment (Kindler et al., 2011) may have reactivated faults and displaced spill points of the buried fluid traps, generating leaking of fluids.

## 6. Conclusions

This work details and quantifies the distribution, the morphology and the vertical architecture of 29 newly discovered abyssal giant pockmarks located at the toe of the BBE; Their origins and the mechanisms leading to their development are discussed consistently to the tectonic setting and the physiography of the area. The results and interpretations can be summarized as follows:

- Pockmarks are all giant (>250 m), abyssal (> 3000 m of water depth) and atypically occurs in carbonate settings below the CCD.
- Pockmarks are all located along the BBE, at less than 5 km from its toe (- 4000 m) and right above a buried carbonate bench related to the BBE erosional retreat.
- Pockmarks are preferentially located where the ocean-continent transition inherited structural lineaments controlling the Black Bahama Escarpment morphology intersect the > 4 km-high submarine carbonate escarpment (BBE).
- The BBE erosional retreat has preferentially reused the inherited faults, initially formed during the activity of the transforming ocean-continent transition (such as the Sunniland Fracture zone). Its present shape was mostly acquired by dissolution of carbonates by brines along tectonic structures.

https://doi.org/10.5194/se-2020-11
Preprint. Discussion started: 19 February 2020



- Fluids most probably circulate along the structural heterogeneities of the Bahamian platform, in response to the Kohout convection; Brine (sulfide-rich) formation is related to the dissolution of deep evaporite layers located ~1 km below the seafloor as well as geothermal heating. After oxidation nearby the BBE, the sulfites partially transform into sulphates. This oxidation reaction is indeed favoured by the inflow of oxygenized water through the fractured escarpment. The dense fluids are subsequently laterally trapped into the 5 km wide buried carbonate bench, surrounded by low-permeability hemipelagics, in which the dissolution is over-developed along fractures. The dissolution of the buried bench carbonates implies overlying collapse structures in the fine-grained deposits. In addition, when the critical pressure of the seal of the bench is exceeded, the fluids could be expelled via the bench top and form fluid-escape-features locally piercing fine-grained contourites.

## 7. Acknowledgements

We thank the captain and crew of the R/V *L'Atalante* for the quality of the acquired data, and Ifremer-Genavir (France) for cruise organization and technical support. We thank Mrs. XXXX and Mr. XXXX for their constructive reviews on this manuscript. We acknowledge IHS for granting University of Bordeaux with academic Kingdom® software licences.

## 8. References

Abrams, M.A. and Segall, M.P., Best practices for detecting, identifying and characterizing near-surface migration of hydrocarbons within marine sediments: Offshore Technology Conference in Houston, Texas, 2001. doi.org/10.4043/13039-MS.

Agirrezabala, L. M., S. Kiel, M. Blumenberg, N. Schäfer, and J. Reitner, Outcrop analogues of pockmarks and associated methane-seep carbonates: A case study from Lower Cretaceous (Albian) of the Basque-Cantabrian Basin, western Pyrenees: Palaeogeography Palaeoclimatology, Palaeoecology, 390, 94–115, 2013. doi: 10.1016/j.palaeo.2012.11.020.

Andersen, K. H., T. Lunne, T. J. Kvalstad, and C. F. Forsberg, Deepwater geotechnical engineering, Proc. XXIV National Conference of the Mexican Society of Soil Mechanics, Aguascalientes, 1–57, 2008.

Anderson, E.M., The dynamics of faulting and dyke formation with applications to Britain. Edimburgh., Oliver and Boyd, 206p, 1951.

Backshall, D.G., Barnett, J., Davies, P.J., Duncan, D.C. Harvey, N., Hopley, D., Isdale, P.J., Jennings, J.N. and Moss. R., Drowned dolines – the blue holes of the Pompey Reefs, Great Barrier Reef: Journal of Australian Geology & Geophysics, 4, pp. 99-109, 1979.

Bayon, G., Loncke, L., Dupré, S., Caprais, J.C., Ducassou, E., Duperron, S., Etoubleau, J., Foucher, J.P., Fouquet, Y., Gontharet, S., Henderson, G.M., Huguen, C., Klaucke, I., Mascle, J., Migeon, S., Olu-Le Roy, K., Ondréas, H., Pierre, C., Sibuet, M., Stadnitskaia, A., and Woodside, J., Multi-disciplinary investigation of fluid seepage on an unstable margin: The case of the Central Nile deep sea fan: Marine Geology, 261, pp. 92- 104, 2009.

Betzler, C., Lindhorst, S., Hubscher, C., Ludmann, T., Furstenau, J., and Reijmer, J., Giant pockmarks in a carbonate platform (Maldives, Indian Ocean): Marine Geology, 289, pp.1-16, 2011. doi:10.1016/j.margeo.2011.09.004

Bleifnick, D.M., Robertson, A.H.F., and Sheridan, R.E., Deposition and provenance of Miocene intraclastic chalks, Blake-Bahama Basin, western North Atlantic, in Initial reports of the Deep Sea Drilling Project, Volume 44: Washington, D.C., U.S. Government Printing Office, p. 727-748, 1983.

Carlo, D-L., Characterization of rock-magnetic signature during subaerial exposure in Platform Carbonates from new providence, Bahamas: PhD Thesis, Ohio state University, 66 p., 1996.

Cavailhes T., Sizun J.P., Labaume P., Chauvet A., Buatier B., Soliva R., Mezri L., Charpentier D., Leclere H., Trave A., Gout C., Influence of fault rock foliation on fault zone permeability: The case of deeply buried arkosic sandstones (Grès d'Annot, southeastern France), AAPG Bulletin, 97, 1521-1543, 2013. doi: 10.1306/03071312127.

Chanton, J.P., Martens, C.S., and Paull, C.K., Control of pore-water chemistry at the base of the Florida escarpment by processes within the platform: Nature, 349, pp. 229-231, 1991.

Chapron, E., Van Rensbergen, P., De Batist, M., Beck, C., and Henriet, J.P., Fluid-escape features as a precursor of a large sublacustrine sediment slide in Lake Le Bourget, NW Alps, France: Terra Nova, 16, pp. 305-311, 2004. Doi: 10.1111/j.1365-3121.2004.00566.x

Cole, D., Stewart, S.A. and Cartwright J.A., Giant irregular pockmark craters in the Palaeogene of the Outer Moray Firth Basin, UK North Sea: Marine and Petroleum Geology, 17 pp. 563-577, 2000.

Corbella, M., Ayora, C. Cardellach, E., Hydrothermal mixing, carbonate dissolution and sulfide precipitation in Mississipi valley-type deposits: Mineralium Deposita, 39, p. 344-357, 2004. doi.10.1007/s00126-004-0412-5

Dando, P.R., Austen, M.C., Burke Jr., R.A., Kendall, M.A., Kennicutt II, M.C., Judd, A.G., Moore, D.C., O'Hara, S.C.M., Schmaljohann, R. and Southward, A.J., Ecology of a North Sea pockmark with an active methane seep: Marine Ecology Progress Series, 70, pp. 49–63, 1991.

Dawns, J.M., and Swart, P.K., Textural and geochemical alternations in late Cenozoic Bahamian dolomites: Sedimentology, 35, pp.385-403, 1988.

Dickens, G. R., Rethinking the global carbon cycle with a large, dynamic and microbially mediated gas hydrate capacitor: Earth Planetary Science Letters, 213, pp. 169-183, 2003.

Fauquembergue, K., Ducassou, E., Mulder, T., Hanquiez, V., Perello, M-C, Poli, E., Borgomano, J., Genesis and growth of a carbonate Holocene wedge on the northern Little Bahama Bank: Marine and Petroleum Geology, 96, pp. 602-614, 2018. doi.org/10.1016/j.marpetgeo.2018.05.013

Foland, S., Maher, N., and Yun, J., Pockmarks along the California continental margin; implications for fluid-flow, AAPG Bulletin, 83, 687-688, 1999.

Freeman-Lynde R.P., Cita, M.B., Jadoul, F., Miller, E.L., and Ryan, W. B. F. Marine geology of the Bahama Escarpment: Marine Geology, 44, p. 119-156, 1981.

Freeman-Lynde R.P., and Ryan W.B.F., Erosional modification of Bahama Escarpment: Geological Society of America Bulletin, 96, pp.481-494, 1985.

Garcia-Rios, M., Luquot, L., Soler, J.M., and Cama, J., Influence of the flow rate on dissolution and precipitation features during percolation of CO2-rich sulfate solutions through fractured limestone samples: Chemical Geology: 414, pp. 95–108, 2015.

Garven, Continental-scale groundwater flow and geological processes: Annual Review Earth Planetary Sciences, 23, pp. 89-117, 1995.

Garven, H., and Freeze, R.A., Theorical analysis of the role of groundwater flow in the genesis of stratabound ore deposits; 2, Quantitative results: American Journal of science, 284, 10, pp.1125-1174, 1994. doi: 10.2475/ajs.284.10.1125

Gay A., Lopez M., Cochonat P., Sultan N., Cauquil E. and Brigaud F., Sinuous pockmark belt as indicator of a shallow buried turbiditic channel on the lower slope of the Congo Basin, West African Margin. In: Van Rensbergen P, Hillis RR, Maltman AJ, Morley CK, eds. Subsurface Sediment Mobilization. Special Publications. London: Geological Society of London, pp. 173–189, 2003.

Gay, A., Cavailhes, T., Grauls, D., Marsset, B., Marsset, T., Repeated fluid-expulsions during events of rapid sea-level rise in the Gulf of Lion, western Mediterranean Sea: Bulletin de la Société Géologique de France, 188, 24, 2017. doi: 10.1051/bsgf/2017190.

Gay, A., Lopez, M., Potdevin, J-L, Vidal, V., Varas, G., Favier, A., and Tribovillard, N., 3D morphology and timing of the giant fossil pockmark of Beauvoisin, SE Basin of France: Journal of the Geological Society, 176, pp. 61-77, 2019. DOI: https://doi.org/10.1144/jgs2018-064.

Glaser, J.H., Breathing of the Seafloor: Tidal correlations of seismicity at Axial Volcano: Comment: COMMENT: Geology, 31, 1, e3, 2004. doi.org/10.1130/0091-7613-31.1.e3

Gouze, P., Noiriel, C., Bruderer, C., Loggia, D. and Leprovost, R., X-ray tomography characterization of fracture surfaces during dissolution: Geophysical Research Letter, 2003, 30, 5, pp. 1267, 2003. doi: 10.1029/2002GL016755

Heath K.C., and Mullins H.T., Open-ocean, off-bank transport of fine-grained carbonate sediments in the northern Bahamas. In: Fine-Grained Sediments: Deep- Water Processes and Facies (Ed. by D. A. V. Stow and D. J. W. Piper). Spec. Publ. Geol. Soc. Lond. Blackwell Scientific Publications, Oxford, 15, pp.199-208, 1984. doi.org/10.1144/GSL.SP.1984.015.01.13

Henderson, G. M., Slowey, N., C., and Haddad, G., A., Fluid flow through carbonate platforms: constraints from $^{234}U/^{238}U$ and $Cl^-$ in Bahamas pore-waters: Earth and Planetary Science Letters, 169, pp.99-111, 1999.

Hollister, C.D., Ewing, J.I., Habib, D., Hathaway, J.C., Lancelot, Y., Luterbacher, H., Paulus, F.J., Poag, C.W., Wilcoxon, J.A., and Worstell, P.: Deep Sea Drilling Program Volume XI, Shipboard Site Reports, Site 99, Cat Gap, 1972a. doi:10.2973/dsdp.proc.11.102.1972

Hollister, C.D., Ewing, J.I., Habib, D., Hathaway, J.C., Lancelot, Y., Luterbacher, H., Paulus, F.J., Poag, C.W., Wilcoxon, J.A., and Worstell, P.: Deep Sea Drilling Program Volume XI, Shipboard Site Reports, Site 100, Cat Gap, 1972b. doi:10.2973/dsdp.proc.11.103.1972

Hornbach, M. J., C. Ruppel, and Van Dover C. L., Three-dimensional structure of fluid conduits sustaining an active deep marine cold seep, Geophysical Research Letters, 34, 5, L05601, doi:10.1029/2006GL028859, 2007.

Hugues, J.D., Vacher, H.L. and Sanford W.E., Three-dimensional flow in the Florida platform: Theoritical analysis of Kohout convection at its type locality: The geological Society of America, 35, 7, pp. 663-666, 2007. Doi: 10.1130/G23374A.1.

Kasahara J., Tides, earthquakes, and volcanoes: Science, 297, pp. 348–349, 2002.

Kindler, P., Godefored, F., Chiarada, M., Ehlert, C., Eisenhauer, A., Frank, M., Hasler, C-A., and Samankassou, E., Discovery of Miocene to early Pleistocene deposits on Mayaguana, Bahamas: Evidence for recent active tectonism on the North American Margin: Geology, 39, pp.523-526, 2011.

King, L. H., and MacLean, B., Pockmarks on the Scotian Shelf: Bulletin of the Geological Society of America, 81, pp. 3141–3148, 1970.

Kohout, F.A., Henry, H.R., and Banks, J.E., Hydrogeology related to the geothermal conditions of the Floridan Plateau: Florida Bureau of Geology Special Publication 21, p. 1-39, 1977.

Komatsu, G., Ori, G.G. Cardinale, M., Dohm, M.J., Baker, V.R., Vaz, D.A., Ishimaru, R., Namiki, N. and Matsui, T., Roles of methane and carbon dioxide in geological processes on Mars: Planetary and Space Science, 59, pp. 169-181, 2011.

Maestro, A., Barnolas, A., Somoza, A., Lowrie, A., and Lawton, T., Geometry and structure associated to gas-charged sediments and recent growth faults in the Ebro Delta (Spain): Marine Geology, 186, pp.351-368, 2002.

Marcon, Y., Ondréas, H., Sahling, H., Bohrmann, G., and Olu, K., Fluid-flow regimes and growth of a giant pockmark: Geology, 42, 1, pp.63-66, 2014. doi:10.1130/G34801.1

Masafero, J.L., Bulnes, M., Poblet, J. and Eberli, G.P., Episodic folding inferred from syntectonic carbonate sedimentation: the Santaren anticline, Bahamas foreland: Sedimentary Geology, 146, pp. 11-24, 2002.

Meinen, C., Johns, W., Garzoli, S.L., van Sebille, E., Rayner, D., Kanzow, T., Baringer, O., Variability of the Deep Western Boundary Current at 26.5°N during 2004-2009: Deep-Sea Research II, 85, p.154-168, 2013. doi.org/10.1016/j.dsr2.2012.07.036

Melim, L., and Masaferro, J-L., Subsurface geology of the Bahamas banks. In Vacher, H.L., Quinn, T.M. (Eds), Geology and Hydrogeology of Carbonate Islands. Elsevier Science B.V, Amsterdam, Netherlands, pp.161-182, 1997.

Micallef, A., Bernadt, C., and Debono, G., Fluid flow systems of the Malta Plateau, Central Mediterranean Sea: Marine geology, 284, 1-4, pp. 74-85, 2011.

Michaud, F., Chabert, A., Collot, J-Y., Sallarès, V., Flueh, E.R., Charvis, P., Graindorge, D., Gustcher, M-A. and Billas, J., Fields of multi-kilometer scale sub-scircular depressions in the Carbegie Ridge sedimentary blanket: Effect of underwater carbonate dissolution: Marine Geology, 216, pp. 205-219, 2005.

Michel, G., Dupré, S., Baltzer, A., Ehrhold, A., Imbert, P., Pitel, M., Loubrieu, B., Scalabrin, C., Lazure, P., Marié, L., Geldof. And Deville, E., Pockmarks on the South Aquitaine Margin continental slope: The seabed expression of past fluid circulation and former bottom currents: Comptes Rendus Geoscience, 349, pp. 391-401, 2017.

Morrow, D.W., Regional subsurface dolomitization: models and constraints. Geoscience Canada 25, pp. 57– 70, 1998.

Mulder T., Gillet H., Hanquiez V., Ducassou E., Fauquembergue K., Principaud M., Conesa G., Le Goff J., Ragusa J., Bashah S., Bujan S., Reijmer J.J.G., Cavailhes T., Droxler A.W., Blank D.G., Guiastrennec-Faugas L., Fabregas N., Recouvreur A., Seibert C. Carbonate slope morphology revealing a giant submarine canyon (Little Bahama Bank, Bahamas): Geology, 46, 31-34, 2018, doi: 10.1130/G39527.1.

Mulder T., Gillet H., Hanquiez V., Reijmer J.J.G., Droxler A.W., Recouvreur A., Fabregas N., Cavailhes T., Fauquembergue K., Blank D.G., Guiastrennec-Faugas L., Seibert C., Bashah S., Bujan S., Ducassou E., Principaud M., Conesa G., Le Goff J., Ragusa J., Busson J., and Borgomano J., Into the deep: A coarse-grained carbonate turbidite valley and canyon in ultra-deep carbonate setting, Marine Geology, 407, pp. 316-333, 2019. doi: 10.1016/j.margeo.2018.11.003.

Mullins, H., Breen, N., Dolan, J., Wellner, W., Petruccione, J.L., Gaylord, M., Andersen, B., Melillo, A.J., Jurgens, A.D., Orange, D., Carbonate platforms along the southeast Bahamas-Hispaniola collision zone: Marine Geology, 105, 169-209, 1992.

Mullins, H. T., and Lynts, G.W., Origin of the northwestern Bahama Platform: Review and Reinterpretation: GSA Bulletin, 88, pp. 1447-1461, 1977. doi.org/10.1130/0016-7606(1977)88<1447:OOTNBP>2.0.CO;2

Ondréas, H., Fouquet, K.O, Charlou, J.L., Gay, A., Dennielou, B., Donval, J.P., Fifis, A., Nadalig, T., Cochonat, P., Cauquil, E., Bourillet, J.F., Le Moigne, M. and Sibuet, M., ROV study of a giant pockmark on the Gabon continental margin: Geo-Marine letters, 25, 5, pp. 281-292, 2005.

Orange, D.L., Yun, J., Maher, N, Barry, J, and Greene G., Tracking California seafloor seeps with bathymetry, backscatter and ROVs: Continental Shelf Research, 22(16), pp. 2273–2290, 2002.

Paull C.K., and Dillon, W.P., Erosional origin of the Blake Escarpment: An alternative hypothesis: Geology, 8, pp. 538-542, 1980.

Paull C., and Neumann, A.C., Continental margin brine seeps: Their geological consequences: Geology, 15, pp. 545-548, 1987.

Paull, C.K., Spiess, F.N., Curray, J.R., Twitchell, D., Morphology of Florida Escarpment chemosynthetic brine seep community sites: deep-tow, seabeam, and GLORIA surveys: Conference: Annual meeting of the American Association of Petroleum Geologists, Houston, TX, USA, 20-23 March, 72, 2, 1988

Peterson, M.N. A., Calcite: Rates of dissolution in a vertical profile in the central Pacific: Science, 154, pp. 1542-1544, 1966.

Pilcher, R., and Argent, J., Mega-pockmarks and linear pockmark trains on the West African continental margin: Marine Geology, 244, pp. 15-32, 2007. doi:10.1016/j.margeo.2007.05.002

https://doi.org/10.5194/se-2020-11
Preprint. Discussion started: 19 February 2020



Privalov, V., Randi, A., Sterpenich, J., Pironon, J., and Morlot, C., Structural control of a dissolution network in a limestone reservoir forced by radial injection of CO2 saturated solution; Experimental results coupled with X-Ray computed tomography: Geosciences, 9, 1, 33, 2019.

Post, V. E.A, Groen, J., Kooi, H., Person, M., Ge, S. and Edmunds, W.M., Offshore fresh groundwater reserves as a global phenomenon: Nature, 504, p.p. 71-78, 2013. doi:10.1038/nature12858.

Rollet, N.G.A.L., Kennard, J.M., O'Brien, P.E., Jones, A.T., and Sexton, M., Characterization and correlation of active hydrocarbon seepage using geophysical data sets: An example from the tropical, carbonate Yampi Shelf, Northwest Australia, Marine Petroleum Geology, 23, pp.145-164, 2006.

Rotevatn, A., and Bastesen, E., Fault linkage and damage zone architecture in tight carbonate rocks in the Suez Rift (Egypt): Implications for permeability structure along segmented normal faults, in Spence, G.H., et al., eds., Advances in the Study of Fractured Reservoirs: Geological Society of London Special Publication, 374, pp. 79–95, 2014. doi: 10 .1144 /SP374 .1

Salmi, M.S., Johnson, H.P., Leifer, I. and Keister, J.E., Behavior of methane seep bubbles over a pockmark on the Cascadia continental margin: Geosphere, 7, 6, pp. 1273-1283, 2011. doi: 10.1130/GES00648.1

Sanford, W., and Konikow, L., Porosity development in coastal carbonate aquifers: Geology, 17, pp. 249-252; 1989.

Schlager, W., Austin. J. A., Jr., Corso, W., McNulty, C. L, Fluegel, E., Renz, O., and Steinmetz, J. C., Early Cretaceous platform re-entrant and escarpment erosion in the Bahamas: Geology, 12, pp. 147-150, 1984.

Shaw, J., Courtney, R.C., Currie, J.R., Marine Geology of Saint George's Bay, Newfoundland, as interpreted from multibeam bathymetry and back-scatter data, Geo-Marine Letters, 17, pp. 188-194, 1997.

Sheridan, R.E., Conceptual Model for the Block-fault origin of the North American Atlantic Continental Margin Geoscycline: Geology, 2, 9, pp.465-468, 1974. doi.org/10.1130/0091-7613(1974)2<465:CMFTBO>2.0.CO;2

Sibson, R., Structural permeability of fluid-driven fault-fracture meshes: Journal of structural Geology, 18, 8, pp.1031-1042, 1996. doi: 10.1016/0191-8141(96)00032-6.

Sultan, N., Marsset, B., Ker, S., Marsset, T., Voisset, M., Vernant, A.M., Bayon, G., Cauquil, E., Adamy, J., Colliat, J.L. and Drapeau, D., Hydrate dissolution as a potential mechanism for pockmark formation in the Niger Delta: Journal of Geophysical Research, 115, B08101, 2010. doi:10.1029/2010JB007453

Sun Q., Wu, S., Cartwright, J., and Dong, D., Shallow gas and focused fluid flow systems in the Pearl River Mouth Basin, northern South China Sea: Marine Geology, 1, 14, pp.315-318, 2012

Taylor, M.H., Dillon, W.P. and Pecher, I.A., Trapping and migration of methane associated with the gas hydrate stability zone at the Blake Ridge Diapir: new insights from Seismic data: Marine Geology 164, 79-89, 2000.

Tolstoy M, Vernon F L, Orcutt, J A, and Wyatt, F.K., Breathing of the seafloor: Tidal correlations of seismicity at Axial volcano: Geology, 30, pp. 503–506, 2002

Walles, F.E., Tectonic and diagenetically induced seal failure within the south-western Great Bahamas Bank: Marine and Petroleum Geology, 10, pp. 14-28, 1993.

Whitaker, F.F. and Smart, P.L., Active circulation of saline ground waters in carbonate platforms: Evidence from the Great Bahama Bank: Geology, 18, pp. 200-203, 1990.

Whitaker, F.F., and Smart, P.L., Circulation of saline groundwaters in carbonate platforms: A review and case study from the Bahamas. In: A.D. Horbury and A.G. Robinson (Editors), Diagenesis and Basin Development. Am. Assoc. Petrol. Geol. Studies Geol., 36, pp. 113-132, 1993.

Whitaker, F.F. Smart, P.L., Vahrenkamp, V.C., Nicholson, H. and Wogelius, R.A., Dolomitization by near-normal seawater? Field evidence from the Bahamas. In: B.H. Purser, M. Tucker and D.H. Zenger (editors), Dolomites, A volume in Honour of Dolomieu, International Association of Sedimentology Special Publication, 21, pp.111-132, 1994.

Wierzbicki, R., Dravis, J., Al-Aasnm, Harland, N., Burial dolomitization and dissolution of Upper Jurassic Abenaki platform carbonates, Deep Panuke reservoir, Nova Scotia, Canada: The American Association of Petroleum Geologists, 90, 11, pp. 1843-1861. 2006. DOI: 10.1306/03200605074

Wilson, A.M., Fresh and saline groundwater discharge to the ocean: A regional perspective: Water Resources Research, 41, W02016, doi:10.1029/2004WR003399, 2005.

**9. Figure caption**

https://doi.org/10.5194/se-2020-11
Preprint. Discussion started: 19 February 2020



Figure 1

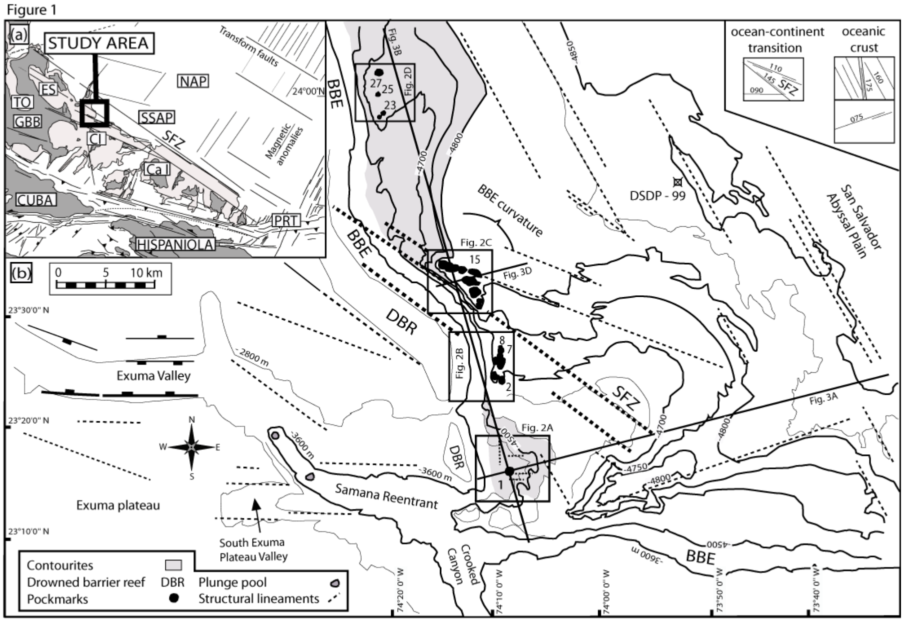


Figure 2

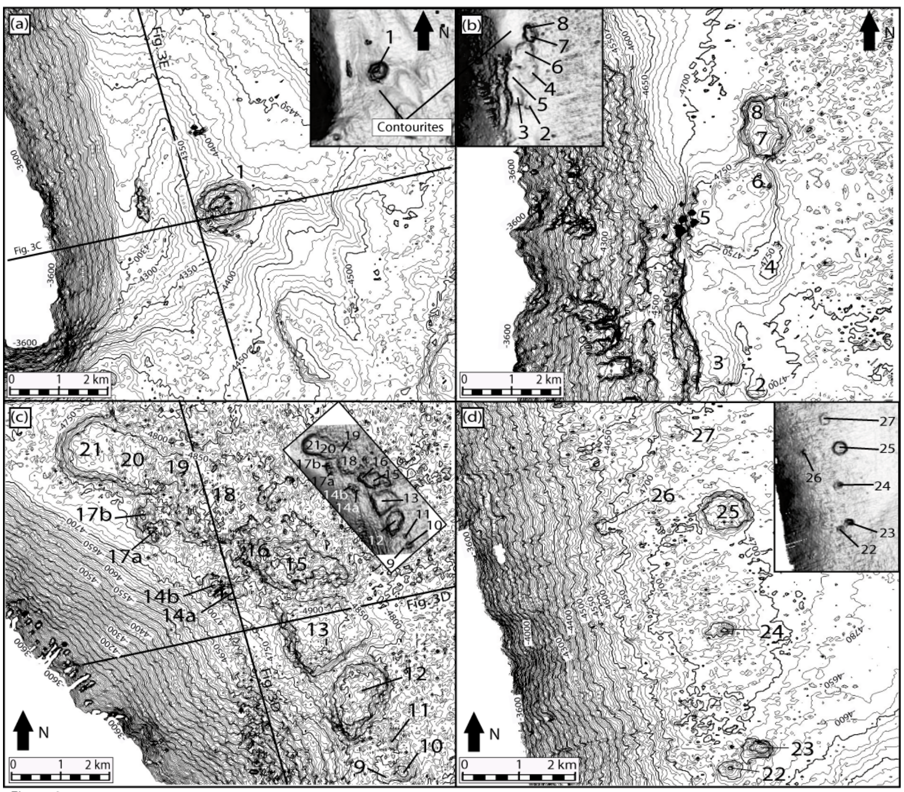

https://doi.org/10.5194/se-2020-11
Preprint. Discussion started: 19 February 2020




**Figure 1. (a) Structural Sketch of the Bahamas, Cuba and Hispaniola region. GGB -> Great Bahama Bank, TO -> Tongue of the Ocean, ES -> Exuma Sound, NP, New Providence, LI, Long Island. SFOZ: Septentrional-Oriente Fault Zone; NHF: North-Hispaniola Fault; SFZ: Sunniland Fracture Zone; NAP: North America Plate; CI Crooked Islands; Ca I: Caicos Islands. SSAB: San Salvador Abyssal Plain. PPT: Puerto Rico Trench. Dark grey is used for both platform water depth < 100 m, and the emerged areas. (b) Physiographic sketch in the Exuma Canyon area where all the pockmarks of this study have been recognized; -3600 m isobath is located within the BBE slope.**

**Figure 2. (a) Details of the Pockmark 1 area where contourites are present. (b) Details of the pockmark 2 to 8 area where inner chains and outer chains appear. (c) Details of pockmarks 9 to 21 area within the BBE curvature where inner and outer chains have been identified. (d) Details of the pockmark 22 to 27 area. Slope maps are also provided for each bathymetric map.**

https://doi.org/10.5194/se-2020-11
Preprint. Discussion started: 19 February 2020

Solid Earth
Discussions
Open Access
EGU

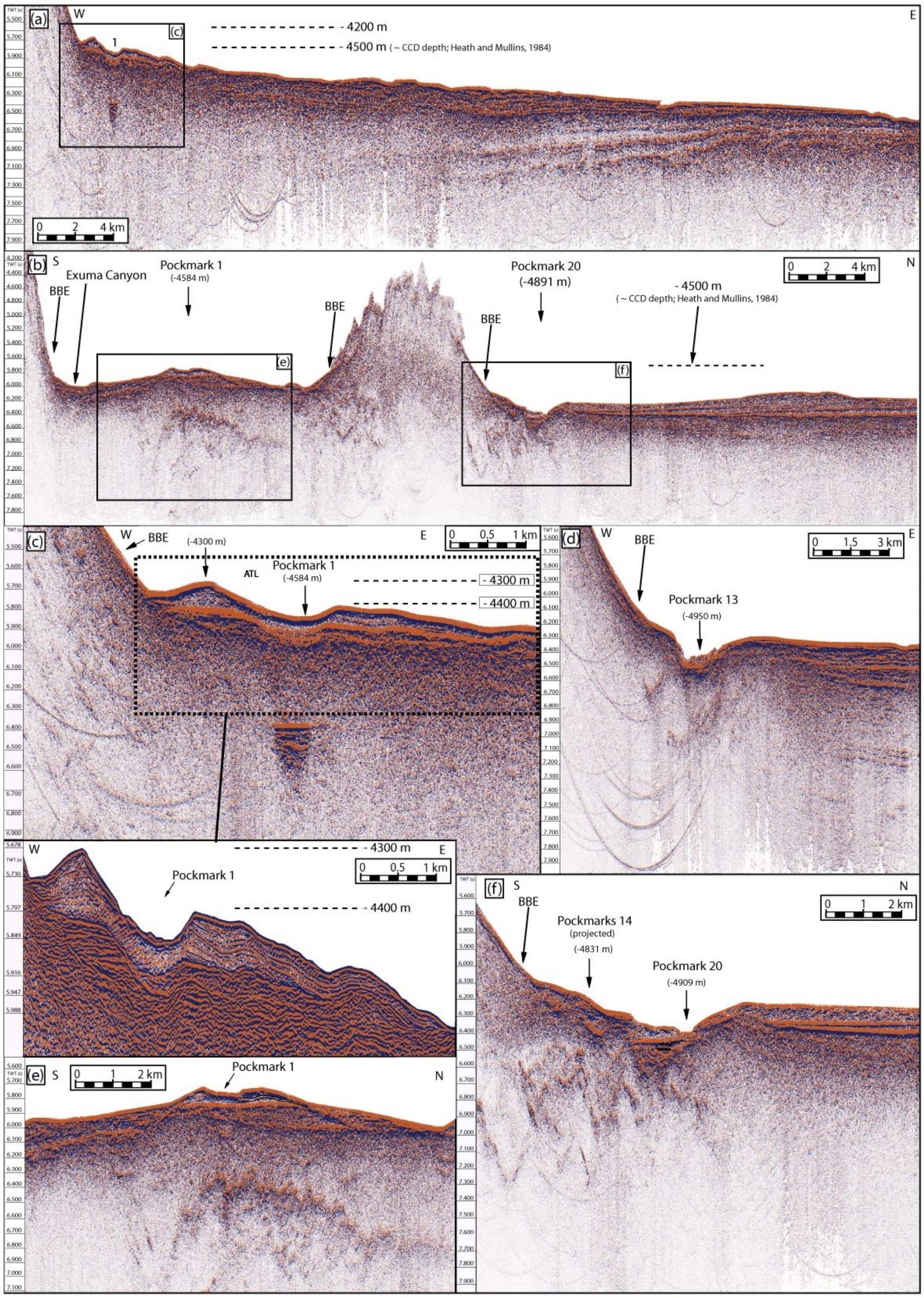

https://doi.org/10.5194/se-2020-11
Preprint. Discussion started: 19 February 2020


Solid Earth Discussions

**Figure 3: 2D seismic lines TWT (s) of the study area: (a) N080 trending line respectively showing from the west (left) to the east (right) the BBE, the pockmark #1 and the San Salvador Abyssal Plain. (b) N170 trending line respectively showing respectively from the south (left) to the north (right), the Exuma Canyon, the pockmark #1, the BBE, the pockmark #2 and the layered northern contouritic deposits. (c) Details of (a) showing the pockmark #1 with its underlying seismic anomaly. (d) N080-trending line crossing the pockmark #13 in the BBE curvature area. (e) Details of (b) showing the pockmark #1 with its related underlying seismic anomaly. (f) Details of (b) showing the pockmark 20 in the BBE curvature area. The aforementioned seismic lines are also reported in Figure 2.**

https://doi.org/10.5194/se-2020-11
Preprint. Discussion started: 19 February 2020


867
868

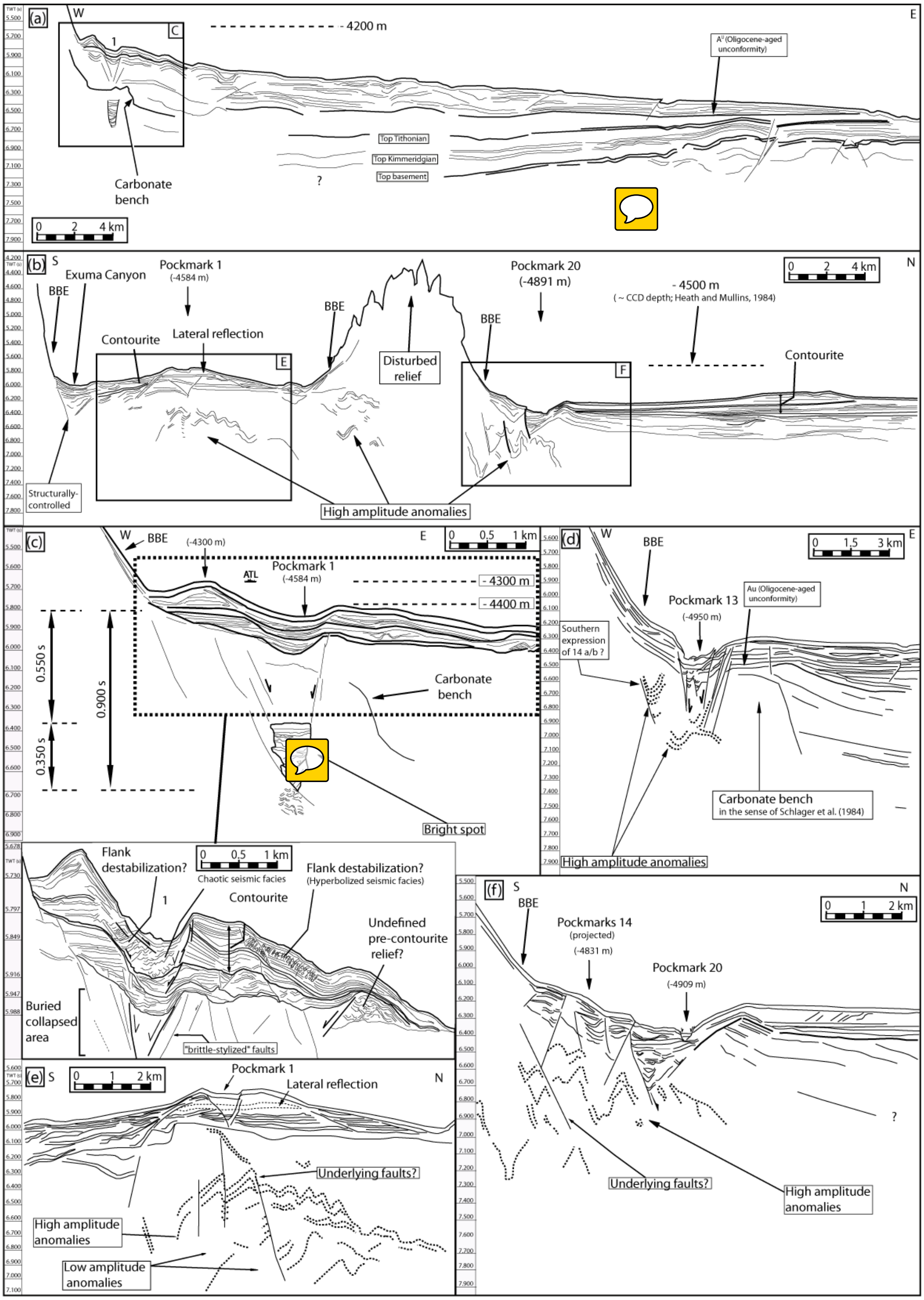

https://doi.org/10.5194/se-2020-11
Preprint. Discussion started: 19 February 2020




**Figure 4: Interpreted 2D seismic lines of the study area: (a) N080 trending line interpretation showing the top basement, the top Kimmeridgian, the top Tithonian, the A[u] unconformity and the post Miocene deposits. (b) N170 trending line interpretation showing the southern contouritic deposits where the pockmark #1 is located, the layered northern contouritic deposits and the pockmark underlying seismic anomalies. (c) Interpreted details of (a) showing the pockmark #1, piercing the contouritic deposits, the related underlying faults and seismic anomalies. (d) Interpreted N080 trending line crossing the pockmark #13 and showing the underlying seismic anomalies as well as the related collapse faults. (e) Interpreted details of (b) showing the lateral reflection within the pockmark #1 piercing the contouritic deposits as well as its underlying seismic anomaly. (f) Interpreted details of (b) showing the normal faults probably related to the pockmark formation in the BBE curvature area.**
**The aforementioned seismic lines are also reported in Figure 2.**

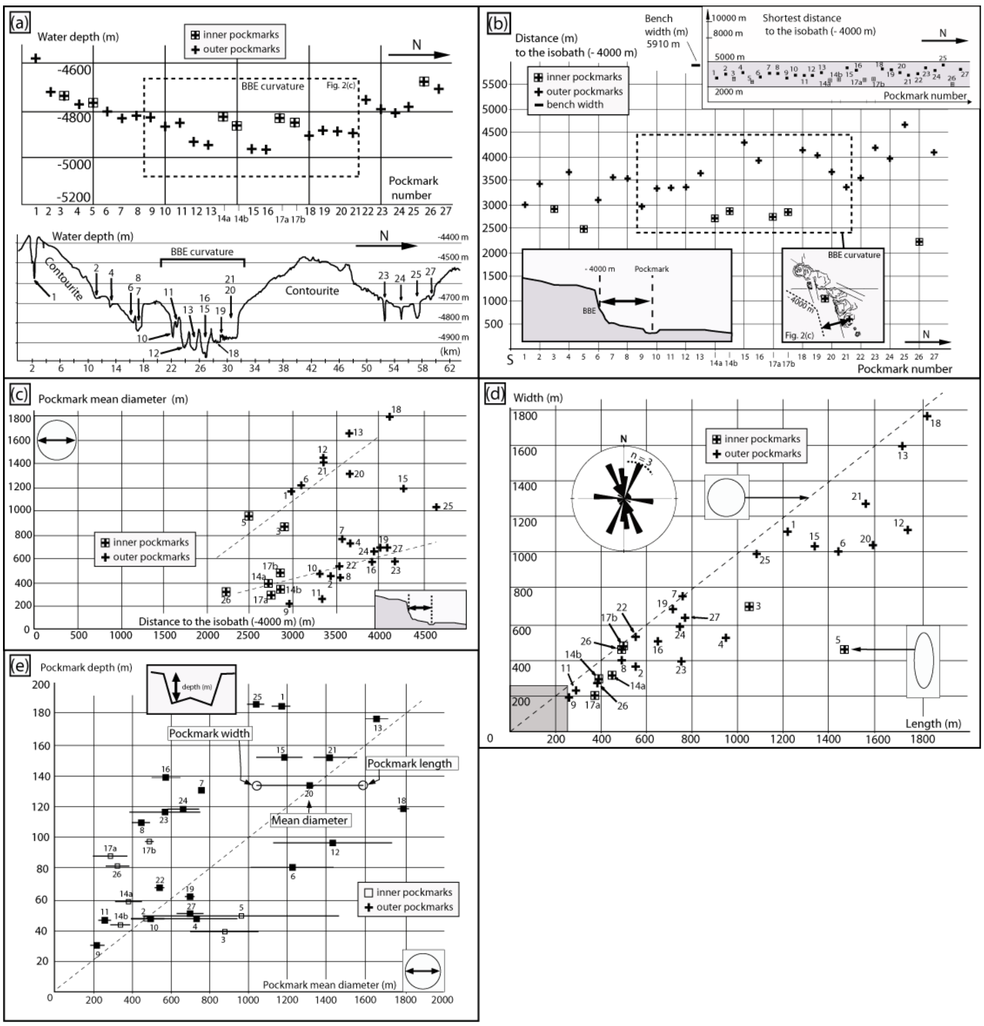

https://doi.org/10.5194/se-2020-11
Preprint. Discussion started: 19 February 2020



**Figure 5: Graphs showing (a) the water depth for the 29 pockmarks of this study and a related S-N bathymetric profile crossing the outer pockmarks. (b) S-N pockmarks numbering as a function of the distance to the BBE, here expressed by the isobath (-4000 m). (c) Pockmark mean diameter as a function of the shortest distance to the BBE. (d) Pockmark width as a function of pockmark length. Related rose diagram showing the elongation trend in the study area. (e) Pockmark depth as a function of the pockmark mean diameter.**

https://doi.org/10.5194/se-2020-11
Preprint. Discussion started: 19 February 2020

Solid Earth
Discussions

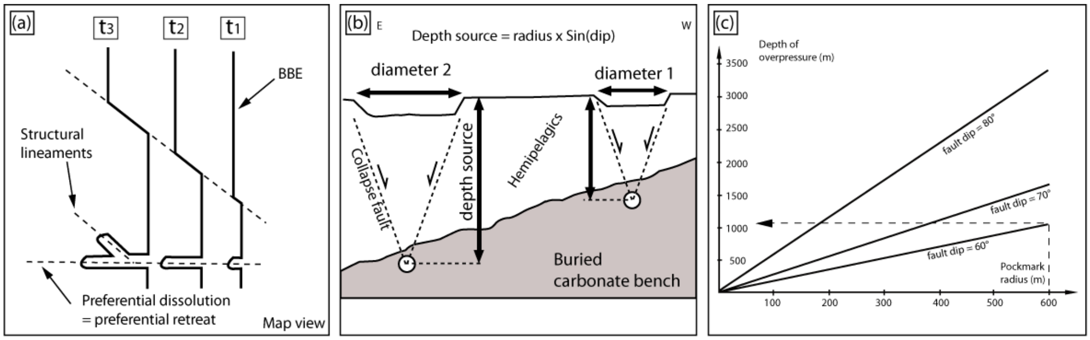


Figure 6

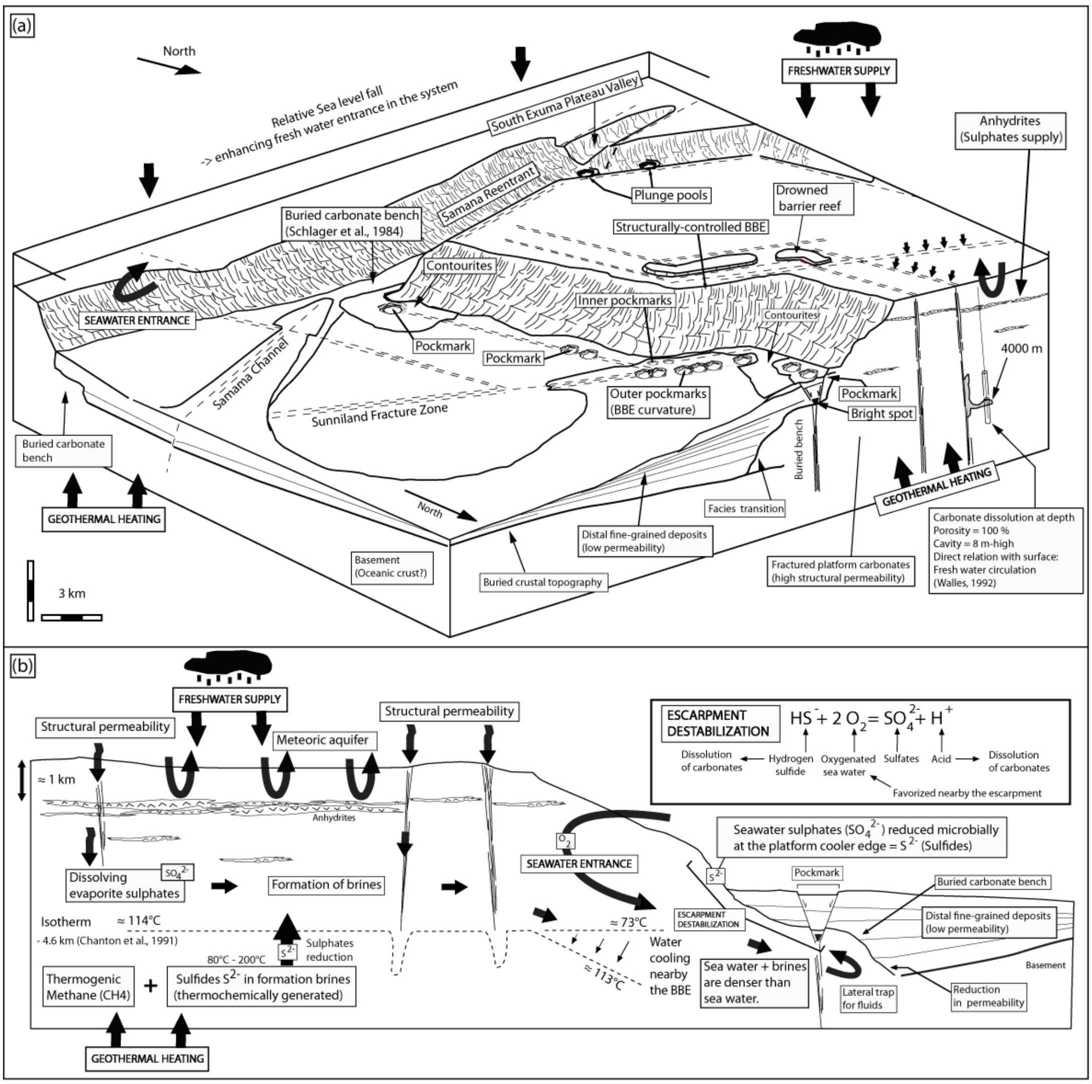


Figure 7

https://doi.org/10.5194/se-2020-11
Preprint. Discussion started: 19 February 2020

Solid Earth Discussions

**Figure 6: (a) Conceptual sketch showing how the BBE erosional retreat probably use the structural lineaments related to the TOC transition to reach its present-day physiography. (b) Conceptual sketch showing the relations between the depth of the fluid source and the radius of outer and inner pockmarks (c) Quantitative estimation of the overpressure depth in the case of pockmark 1.**

**Figure 7: (a) 3D block diagram expressing the general understanding of the system including our observations and the previous literature understanding. (b) 2D understanding of the system showing the importance of temperature, chemistry, and structural/sedimentological geometries.**

| POCKMARK NUMBER (From N to S) | WATER DEPTH (m) | POCKMARK DEPTH (m) | DISTANCE (m) TO THE ISOBATH "-4000 m" | LENGTH (m) | LENGTH (°N) ORIENTATION | WIDTH (m) | WIDTH (°N) ORIENTATION | MEAN DIAMETER (m) |
|---|---|---|---|---|---|---|---|---|
| 1 | -4584 | 184 | 2965 | 1213 | 42 | 1115 | 132 | 1164 |
| 2 | -4722 | 47 | 3428 | 548 | 20 | 357 | 110 | 452,5 |
| 3 | -4739 | 39 | 2894 | 1045 | 159 | 697 | 249 | 871 |
| 4 | -4772 | 47 | 3650 | 940 | 25 | 520 | 115 | 730 |
| 5 | -4771 | 49 | 2474 | 1461 | 179 | 454 | 269 | 957,5 |
| 6 | -4803 | 80 | 3087 | 1433 | 24 | 1008 | 114 | 1220,5 |
| 7 | -4841 | 130 | 3563 | 756 | 176 | 753 | 266 | 754,5 |
| 8 | -4824 | 109 | 3538 | 489 | 85 | 396 | 175 | 442,5 |
| 9 | -4834 | 30 | 2943 | 255 | 154 | 183 | 244 | 219 |
| 10 | -4871 | 47 | 3307 | 487 | 170 | 455 | 260 | 471 |
| 11 | -4851 | 46 | 3336 | 288 | 151 | 223 | 241 | 255,5 |
| 12 | -4933 | 96 | 3341 | 1733 | 22 | 1125 | 112 | 1429 |
| 13 | -4950 | 176 | 3638 | 1712 | 144 | 1599 | 234 | 1655,5 |
| 14a | -4830 | 58 | 2709 | 447 | 151 | 312 | 241 | 379,5 |
| 14b | -4866 | 43 | 2842 | 388 | 145 | 288 | 235 | 338 |
| 15 | -4966 | 151 | 4268 | 1330 | 93 | 1034 | 183 | 1182 |
| 16 | -4967 | 138 | 3898 | 643 | 36 | 500 | 126 | 571,5 |
| 17a | -4835 | 87 | 2736 | 371 | 162 | 198 | 252 | 284,5 |
| 17b | -4857 | 97 | 2838 | 495 | 72 | 470 | 162 | 482,5 |
| 18 | -4909 | 118 | 4114 | 1819 | 168 | 1765 | 258 | 1792 |
| 19 | -4886 | 61 | 4011 | 710 | 93 | 680 | 183 | 695 |
| 20 | -4891 | 133 | 3648 | 1584 | 172 | 1038 | 262 | 1311 |
| 21 | -4897 | 151 | 3339 | 1552 | 22 | 1273 | 112 | 1412,5 |
| 22 | -4757 | 67 | 3525 | 547 | 60 | 527 | 150 | 537 |
| 23 | -4797 | 116 | 4171 | 748 | 90 | 385 | 180 | 566,5 |
| 24 | -4812 | 118 | 3928 | 741 | 95 | 581 | 185 | 661 |
| 25 | -4785 | 185 | 4648 | 1075 | 118 | 993 | 208 | 1034 |
| 26 | -4681 | 81 | 2211 | 381 | 8 | 266 | 98 | 323,5 |
| 27 | -4710 | 50 | 4079 | 762 | 152 | 630 | 242 | 696 |

**Table 1: Quantification of pockmarks attributes**